

Crystal Structure of Polyhedral Oligomeric Silsesquioxane (POSS) Nano-materials: A Study by X-ray Diffraction and Electron Microscopy

Alan. J. Waddon*[†] and E. Bryan Coughlin*[‡]

Department of Polymer Science and Engineering, University of Massachusetts,
Amherst, Massachusetts 01003

Received May 1, 2003. Revised Manuscript Received August 20, 2003

The crystal structure and morphology of inorganic–organic hybrid POSS nanoparticles, consisting of an inorganic core of silicon and oxygen and outer organic attachments of alkyl groups, has been studied using X-ray diffraction and electron microscopy. These molecules self-assemble to form a hexagonally packed structure. Alkyl attachments are accommodated within the interstices of the hexagonal lattice. The results have implications for our understanding of the disorder in polymer–POSS nanocomposite materials such as those formed by copolymerization.

Introduction

Molecular nanocomposites are generating tremendous attention and excitement in the materials community. Such materials offer the prospect of improving the engineering properties of conventional materials and creating new properties. Various types of systems and various approaches to fabrication have been developed. For example, systems based on physical mixtures of clays and polymers have been very widely studied.¹ Another class of nanocomposites is based on polyhedral oligomeric silsesquioxane (POSS) molecules which consist of silicon and oxygen atoms arranged in an inner eight-cornered cage, such that the Si atoms are positioned at the corners, as shown schematically in Figure 1.^{2–23} These are receiving enormous current interest, with possible applications as engineering materials and

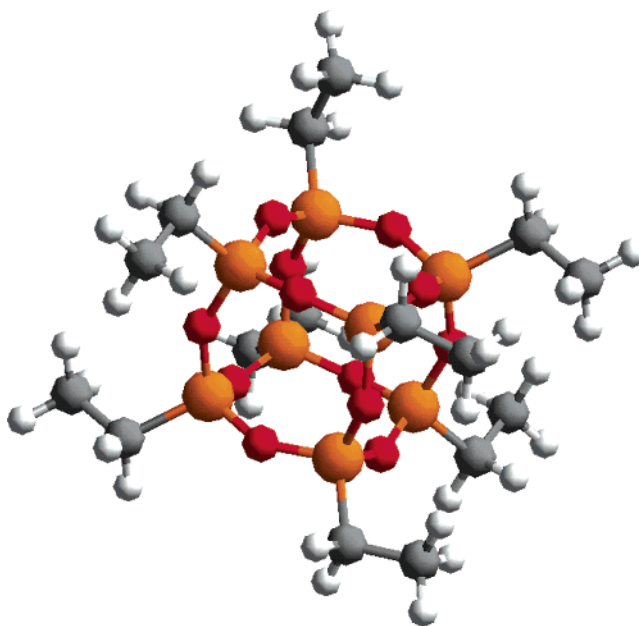


Figure 1. Molecular structure of a POSS molecule with an ethyl attachment at each corner.

* Correspondence may be addressed to either author.

[†] Present address: Department of Engineering Materials, Robert Hadfield Building, University of Sheffield, Sheffield, S1 3JD, Great Britain. E-mail: A.Waddon@sheffield.ac.uk.

[‡] E-mail: coughlin@mail.pse.umass.edu.

(1) Giannelis, E. P. *Adv. Mater.* **1996**, *8*, 29. LeBaron, P. C.; Wang, Z.; Pinnavaia, T. J. *Appl. Clay Sci.* **1999**, *15*, 11. Oriakhi, C. O. *J. Chem. Ed.* **2000**, *77*, 1138. Garces, J. M.; Moll, D. J.; Bicerano, J.; Fibiger, R.; McCleod, D. G. *Adv. Mater.* **2000**, *12*, 1835.

(2) Lichtenhan, J. D. In *Polymeric Materials Encyclopedia*; Salamone, J. C., Ed.; CRC Press: Boca Raton, FL, 1996; p 7768.

(3) Schwab, J. J.; Lichtenhan, J. D. *Appl. Organomet. Chem.* **1998**, *12*, 707.

(4) Lichtenhan, J. D.; Vu, N. Q.; Carter, J. A.; Gilman, J. W.; Feher, F. J. *Macromolecules* **1993**, *26*, 2141.

(5) Lichtenhan, J. D.; Otonari, Y. A.; Carr, M. J. *Macromolecules* **1995**, *28*, 8435.

(6) Haddad, T. S.; Lichtenhan, J. D. *Macromolecules* **1996**, *29*, 7302.

(7) Lee, A.; Lichtenhan, J. D. *Macromolecules* **1998**, *31*, 4970.

(8) Romo-Uribe, A.; Mather, P. T.; Haddad, T. S.; Lichtenhan, J. D. *J. Polym. Sci., Part B: Polym. Phys.* **1998**, *36*, 1857.

(9) Lee, A.; Lichtenhan, J. D. *J. Appl. Polym. Sci.* **1999**, *73*, 1993.

(10) Mather, P. T.; Jeon, H. G.; Romo-Uribe, A.; Haddad, T. S.; Lichtenhan, J. D. *Macromolecules* **1999**, *32*, 1194.

(11) Shockey, E. G.; Bolf, A. G.; Jones, P. F.; Schwab, J. J.; Chaffee, K. P.; Haddad, T. S.; Lichtenhan, J. D. *Appl. Organomet. Chem.* **1999**, *13*, 311.

(12) Fu, B. X.; Zhang, W. H.; Hsiao, B. S.; Rafailovich, M.; Sokolov, J.; Johansson, G.; Sauer, B. B.; Phillips, S.; Balsani, R. *High Perform. Polym.* **2000**, *12*, 565.

(13) Hsiao, B. S.; White, H.; Rafailovich, M.; Mather, P. T.; Jeon, H. G.; Phillips, S.; Lichtenhan, J.; Schwab, J. *Polymer* **2000**, *41*, 437.

fire-resistant materials.^{15,23} This family of materials is of concern here.

Nano-structured materials based on POSS differ from other nano-fillers in a number of respects. Structurally,

(14) Fu, B. X.; Hsiao, B. S.; Pagola, S.; Stephens, P.; White, H.; Rafailovich, M.; Sokolov, J.; Mather, P. T.; Jeon, H. G.; Phillips, S.; Lichtenhan, J.; Schwab, J. *Polymer* **2001**, *42*, 599.

(15) Mantz, R. A.; Jones, P. F.; Chaffee, K. P.; Lichtenhan, J. D.; Gilman, J. W.; Ismail, I. M. K.; Burmeister, M. J. *Chem. Mater.* **1996**, *8*, 1250.

(16) Zheng, L.; Farris, R. J.; Coughlin, E. B. *Macromolecules* **2001**, *34*, 8034.

(17) Zheng, L.; Waddon, A. J.; Farris, R. J.; Coughlin, E. B. *Macromolecules* **2002**, *35*, 2375.

(18) Waddon, A. J.; Zheng, L.; Farris, R. J.; Coughlin, E. B. *Nano Lett.* **2002**, *2*, 1149.

(19) Bharadwaj, R. K.; Berry, R. J.; Farmer, B. L. *Polymer* **2000**, *41*, 7209.

POSS units are precisely defined by their molecular architecture, unlike other nano-fillers which can be relatively imprecisely defined structural units with distributions in both size and shape. The inner cage can be represented as $(\text{SiO}_{1.5})_8$ and is ~ 0.45 nm in diameter. An additional attractive characteristic is the ability to "tailor" properties of the molecule by attaching a variety of functional groups to the corners of the cage via the tetravalent Si atoms. Changing the nature and/or the size of the functional unit allows the generation of an enormous number of POSS-based molecules with outer units of different character. Figure 1 shows a representation of a POSS molecule with ethyl attachments at all eight corners. Appropriate choice of the outer groups confers a wide range of "tailored-in" properties to the molecule. For example, the surface properties and the miscibility behavior can be changed by the choice of hydrophobic or hydrophilic attachments.

One of the most exciting applications of molecular "tailoring" is the possibility of incorporating one (or more) chemically reactive group to specific corners of the cage to provided sites for further chemical reaction. This allows the POSS unit to be covalently incorporated into larger molecules, for instance, as a terminal group on a linear organic chain, or as a comonomer for polymerization with a second monomer unit to form a copolymer in which POSS units are attached as pendant groups. A variety of POSS-containing copolymers,²⁰ including polyethylene,¹⁶ polyurethane,¹² epoxy thermosets,²² and polybutadiene have been prepared by this approach and represent a new generation of polymeric materials lying at the interface of organic and inorganic materials.¹⁵ These copolymers can have superior mechanical properties (modulus, strength, etc.), higher glass transition temperatures, and superior fire resistance than the corresponding homo-polymer.

Clearly, the improvements in polymer properties are related to the structural changes (at all levels) caused by the introduction of the pendant groups. In the monomeric state, POSS molecules are highly crystalline and, in many cases, crystalline domains of POSS are also found in copolymers.^{12,17} It has also been demonstrated that crystallization of POSS in a copolymer can be appreciably suppressed by suitable processing.¹⁸ Whether the observed molecular reinforcement is derived from aggregation of POSS or whether it is caused simply by the bulkiness of individual POSS units, as suggested by some molecular simulations,¹⁹ is not entirely resolved. However, there is experimental evidence that the polymer thermo-oxidative stability is increased by crystallization of POSS pendant groups.^{18,23}

To properly understand and modify the crystalline structure and texture in POSS-based nanomaterials, it is necessary to carefully consider the details of the crystalline structures of POSS. This is the purpose of the present work. Importantly, the essential features of the X-ray diffraction fingerprints of polymerized

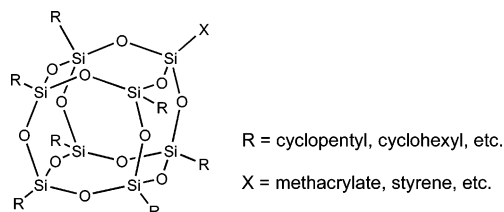


Figure 2. Generalized representation of POSS monomer in which one corner attachment can be used for further reaction.

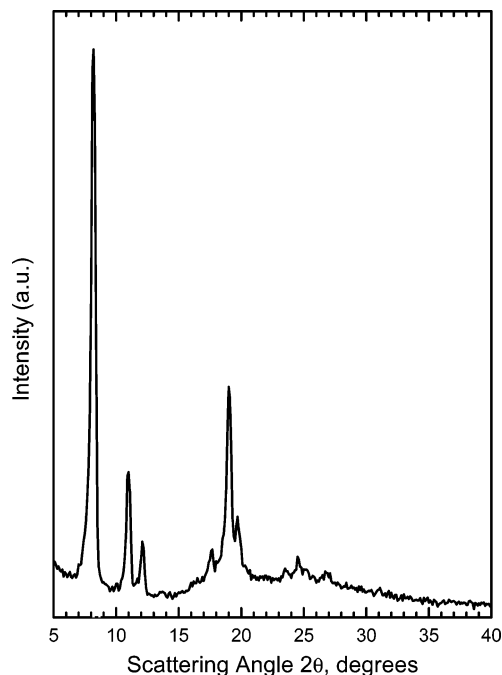


Figure 3. Diffractogram of POSS cyclopentyl-norbornyl monomer. (Powder diffraction from this monomer has been previously reported in ref 18.)

systems are essentially the same as those of the free POSS, indicating the same basic structural characteristics, albeit with a considerable degree of disorder^{12,17,18} in the polymeric system. The approach chosen was to examine the crystal structure and morphology of one specific POSS monomer with alkyl attachments using X-ray and electron microscopy methods. The crystal structure is then compared with literature reports of other POSS monomers to establish general trends for this class of related materials.

Experimental Section

Figure 2 shows the generalized molecular structure of the POSS monomer used experimentally. In the specific case of our experimental material seven corner groups are cyclopentyl and one is a norbornyl group. The material was obtained from the Air Force Research Laboratory, Propulsion Directorate Edwards Air Force Base. The crystal structure and crystal morphology were investigated using powder X-ray diffraction and transmission electron microscopy (TEM). Diffractometry was carried out with as-received material without further preparation with a Siemens D500 diffractometer in transmission mode and $\text{Cu K}\alpha$ radiation. The scan range of 2θ was 5° – 40° with a step interval of 0.1° . Crystals were prepared for TEM by drying a solution of POSS in xylene on carbon film supported on copper TEM grids. Samples were shadowed with gold and TEM was performed with a JEOL 100CX instrument operating at 100 kV.

(20) Li, G.; Wang, L.; Ni, H.; Pittman, C. U. *J. Inorg. Organomet. Polym.* **2001**, *11*, 123.

(21) Baney, R. H.; Itoh, M.; Sakakibara, A.; Suzuki, T. *Chem. Rev.* **1995**, *95*, 1409.

(22) Choi, J.; Harcup, J.; Yee, A. F.; Zhu, Q.; Laine, R. M. *J. Am. Chem. Soc.* **2001**, *123*, 11420.

(23) Gonzalez, R. I.; Phillips, S. H.; Hoflund, G. B. *J. Spacecrafts Rockets* **2000**, *37*, 463.

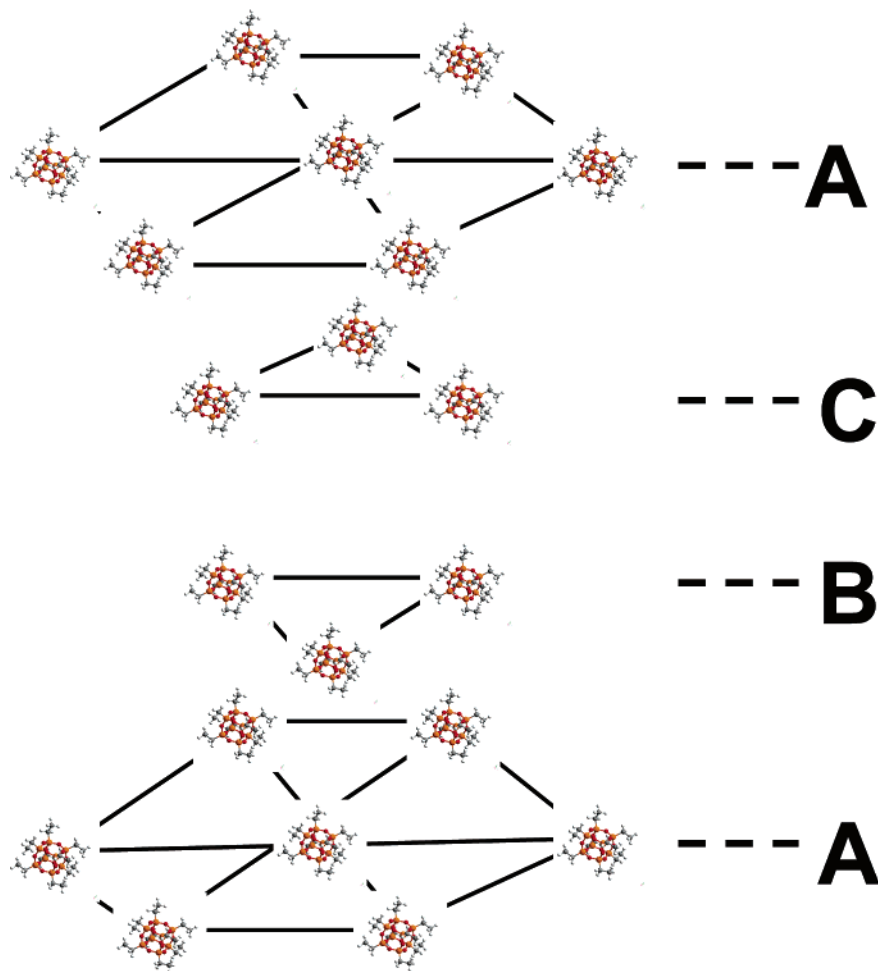


Figure 4. Schematic of hexagonally packed POSS molecules. The sequence of packing in adjacent layers is ABCA. This figure is purely schematic and the distances within the structure as drawn are not intended to be representative of the values in the real crystal.

Results and Discussion

A powder diffractogram is reproduced here in Figure 3. The main features of this are summarized in Table 1 and show four main reflections at 8.2° , 11.0° , 12.1° , and 19.0° , which correspond to lattice spacings of 10.8, 8.03, 7.31, and 4.66 Å, respectively. The diffraction spectrum is very similar to those recently reported for other POSS molecules.¹² Importantly, there is also an older body of work by Larsson and co-workers on the details of crystal structures of a variety of POSS monomers with alkyl attachments.^{24–26} Significantly, Larsson's work, using single-crystal X-ray diffraction, indicates that, in all of the alkyl silsesquioxane structures, the molecules pack in approximately spherical structures. Moreover, this work shows that the structures in this family of molecules have features which are also shared by the new POSS materials. The papers by Larsson can therefore be used as a starting point for the present discussion.

The eight cornered central cages arrange in one plane on a hexagonal array. These cages can be regarded as being approximately spherical. The three-dimensional structure is achieved by stacking such hexagonally

Table 1. X-ray Diffraction Reflections for Cyclopentyl/Norbornyl Corner Attachments

2θ (deg)	d -spacing (Å)	hkl	intensity
8.2	10.8	101, $\bar{1}11$	VS
11.0	8.03	$110, \bar{2}10, \bar{2}10$	S
12.1	7.31	$\bar{1}02, 012$	M
19.0	4.66	$113, \bar{2}13, \bar{1}23$ 300, 330	VS

packed planes in ABCA sequence such that each fourth layer lies exactly above the first layer,²⁴ as shown schematically in Figure 4. Packing of the cages in the hexagonal array is rather open and far from close-packed. Side groups are accommodated around the spherical centers, separating cages within the hexagonal plane and also forcing apart adjacent planes.

Crystallographically, the resulting structure can be described as either hexagonal or rhombohedral. The hexagonal cell contains three molecules and is defined by a_{hex} and c_{hex} . The rhombohedral cell is a one molecule primitive cell and is defined by a_{rh} and α_{rh} . Figure 5 shows the relationship between the cells. The hexagonal cell, although nonprimitive, is considered to be more convenient and to better convey the physical characteristics of the molecular packing and will be used here.

The space group reported by Larsson for the systems he studied was $R\bar{3}$. For this space group permitted

(24) Larsson, K. *Ark. Kemi* **1960**, *16*, 203.

(25) Larsson, K. *Ark. Kemi* **1960**, *16*, 209.

(26) Larsson, K. *Ark. Kemi* **1960**, *16*, 215.

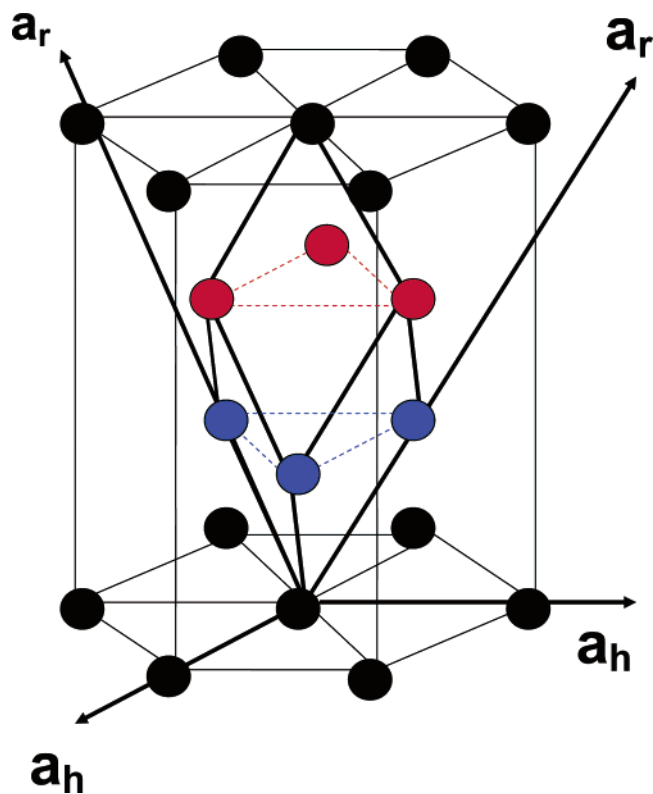


Figure 5. Relationship between hexagonal and rhombohedral cells. (The dimensions in the drawn cell are not intended to represent the actual dimensions in any of the POSS structures.)

reflections (from the hexagonal cell) must satisfy the criterion:

$$-h + k + l = 3n \quad (\text{where } n \text{ is } 0, 1, 2, \text{ etc.})$$

In the rhombohedral system, because the cell is a one motif structure, no reflections are forbidden.

The major reflections in Figure 3 can be indexed as in Table 1. This indexing is also appropriate for the monomer of ref 12.

In the hexagonal system, equivalent planes do not necessarily have the same form of Miller indices.²⁷ In Table 1 planes (101) and ($\bar{1}11$) are equivalent (as are (110), ($\bar{2}10$), and ($2\bar{1}0$); ($\bar{1}02$) and (012); (113), ($\bar{2}13$), and ($\bar{1}23$); and (300) and (330)). The first three reflections in Table 1 are therefore from unique planes. The (113)/($\bar{2}13$)/($\bar{1}23$) planes, however, are not equivalent to (300)/(330). The reflection at 4.66 Å is therefore actually comprised of two overlapping reflections of slightly different spacings.

The indexing of these reflections allows a and c to be evaluated at 16.06 and 17.14 Å, respectively. From these values a number of physically significant parameters can be determined. These are (i) the distance between rows of molecules within the hexagonal basal plane, given by $d_{100} = a \sin 60^\circ$ (=13.9 Å), (ii) the distance between adjacently stacked basal planes, given

by d_3 (=5.71 Å), (iii) the projected area of one molecule on the basal plane, given by $a^2 \sin 60^\circ$, (iv) the ratio of d/a . The value of the a parameter is a measure of how closely cages pack within the hexagonal basal plane, while the c parameter is a measure of the closeness of packing between adjacent hexagonal planes. The ratio between these (d/a) can therefore be understood as an indication of the comparative packing efficiencies within the basal plane and between the adjacent basal planes.

Table 2 compares these values for this molecule with those for other comparable POSS-based molecules also decorated with alkyl attachments (taken from the literature). In all these cases the (SiO_{1.5})₈ central cage is identical: differences are in size and nature of the alkyl corner units. The size and bulkiness of the groups increase toward the bottom of the table.

Inspection of this table reveals some important trends. For all the family (including corner groups consisting of simply hydrogen atoms), parameters dependent only on a (i.e., d_{100} and projected area on basal plane) increase with the size/bulkiness of the corner units. The value of c initially decreases from hydrogen to methyl side units, but then generally increases. For close packing of spheres in ABCA sequence the theoretical value of d/a is 2.45. In all the examples of hexagonally packed POSS the d/a ratio is substantially smaller than this. The physical interpretation of this is that the packing of molecules within the basal planes is relatively open compared to separation between planes. As expected, close packing is approached most closely when the corner units are simply hydrogen atoms, indicated by the larger d/a ratio. Particularly interesting is the observation that, in all other cases, d/a appears to reach a constant ratio of ~ 1.03 , even though attachments consist of variously sized alkyl groups and cyclo-alkyl groups and also when one of the corner groups is replaced by a distinctly different group. This implies that the molecular arrangement within the various crystals is essentially similar in all these cases.

In the ABCA stacking sequence, cages in one layer are positioned above interstitial spaces in adjacent layers (Figure 4). For close packing of hard spheres, the interstitial spaces are small and shallow, forcing neighboring layers apart, such that $d/a = 2.45$. If, however, the basal plane is not close-packed, interstitial spaces are larger and adjacent layers can approach each other more closely, reflected in a corresponding decrease in d/a . For all materials with attachments larger than hydrogen atoms, the approximately constant d/a ratio indicates corner groups are accommodated within the structure in similar ways. In the specific case of hydrogen attachments, corner groups are clearly very small and the molecule most closely approximates to spherical. Accordingly, the a value is also smallest, consistent with the closest packing on the basal plane. However, it is also noted that c is unusually large, suggesting that the closer packing on the basal plane produces smaller and shallower interstitial spaces, therefore forcing larger separations between adjacent planes.

It is emphasized that the above discussion applies only when corner attachments are alkyl. Importantly, Larsson found that if aryl units were attached at the

(27) This confusing situation in which crystallographically equivalent planes have different forms of indices can be avoided by the use of Miller-Bravais indices ($hkil$), in the hexagonal system. However, some confusion in the POSS literature has already been caused by the use of hexagonal and rhombohedral indices, and the introduction of a third system is not considered to be helpful.

Table 2. Crystal Structural Parameters for POSS with Alkyl Corner Attachments

	ref	a (Å)	c (Å)	d_{100} (Å)	$c/3$ (Å)	$a^2 \sin 60^\circ$ (Å ²)	ca
(HSiO _{1.5}) ₈	26	9.13	15.36	7.91	5.12	72.2	1.68
(CH ₃ SiO _{1.5}) ₈	24	12.50	13.09	10.83	4.36	135.3	1.05
(C ₂ H ₅ SiO _{1.5}) ₈	25	14.04	14.54	12.16	4.85	170.7	1.04
(nC ₃ H ₇ SiO _{1.5}) ₈	25	15.33	16.44	13.28	5.48	203.5	1.07
(iC ₃ H ₇ SiO _{1.5}) ₈	25	15.40	15.34	13.34	5.11	205.4	1.00
(cyclopentyl) ₇ (norbornyl) (SiO _{1.5}) ₈	17, 18	16.06	17.14	13.91	5.71	223.4	1.07
(cyclo hexyl) ₇ (OSiH(CH ₃) ₂) (SiO _{1.5}) ₈	12	17.06	18.01	14.77	6.00	252.1	1.06
(cyclo hexyl SiO _{1.5}) ₈	12	17.12	18.03	14.83	6.01	253.8	1.05

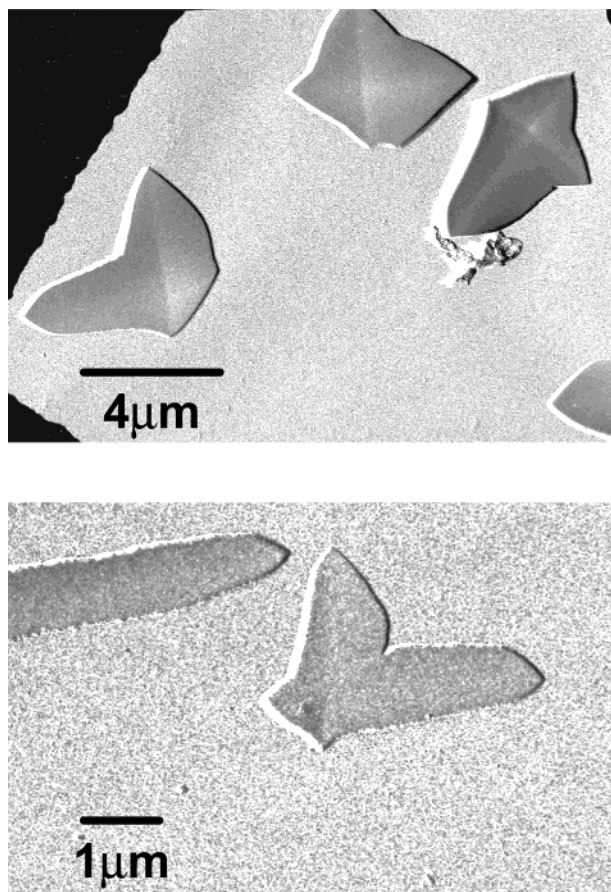


Figure 6. Transmission electron micrographs of crystals of cyclopentyl-norbornyl monomer. Gold shadowed.

corner positions rather than alkyl units, then the symmetry is no longer hexagonal²⁴ (see also ref 28). The role the nature of the side units plays in determining final crystal symmetry is clearly of interest, although beyond the scope of the present study.

Further details of internal crystal structure and its relationship to external crystal shape is provided by transmission electron microscopy and electron diffraction. Figure 6 shows micrographs of the cyclo-pentyl/norbornyl POSS material, crystallized from solution in xylene.

Crystals are platelike, having lateral dimensions on the order of a few micrometers and thickness of a few thousand angstroms. They also show well-defined facets. Crystal growth is often in two approximately orthogonal directions, leading to a four-arm star shape, with arms separated by re-entrant corners. This is a classic indication of crystal twinning. The tips of each arm

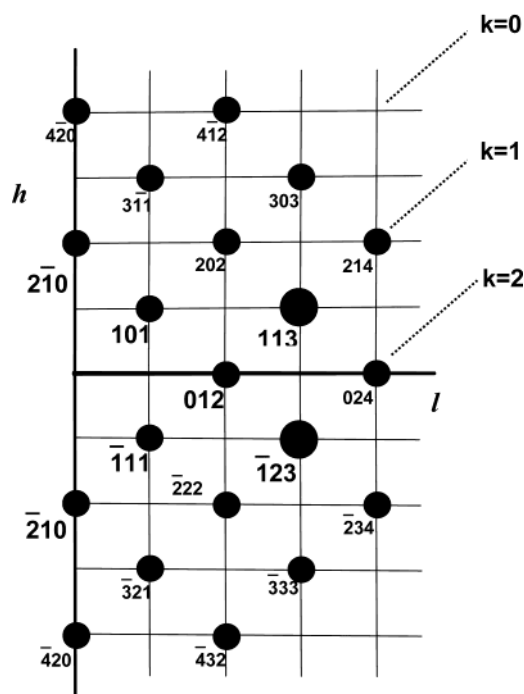
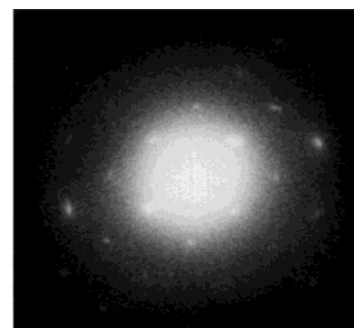


Figure 7. Electron diffraction pattern from crystal of cyclopentyl-norbornyl monomer: (a) experimental pattern; (b) indexed sketch of the right-hand half of the pattern.

commonly end in two facets at approximately 70°. Crystal edges in some cases appear to be curved rather than flat.

A typical electron diffraction pattern (with indexed sketch), taken with the incident beam normal to the plane of the crystal, is shown in Figure 7. This forms an orthogonal pattern. Three of the four most intense reflections can be unambiguously identified as 101 (and equivalent reflections), 210 (and equivalents), and 012 (and equivalents). Figure 7 identifies specific members of the families so that the indexing is self-consistent with 210 and 012 lying on the vertical and horizontal axes, respectively. On the basis of spacing alone the outer intense reflection which occurs at 4.7 Å may be

(28) Feher, F. J.; Budzichowski, T. A. *J. Organomet. Chem.* **1989**, 373, 153.

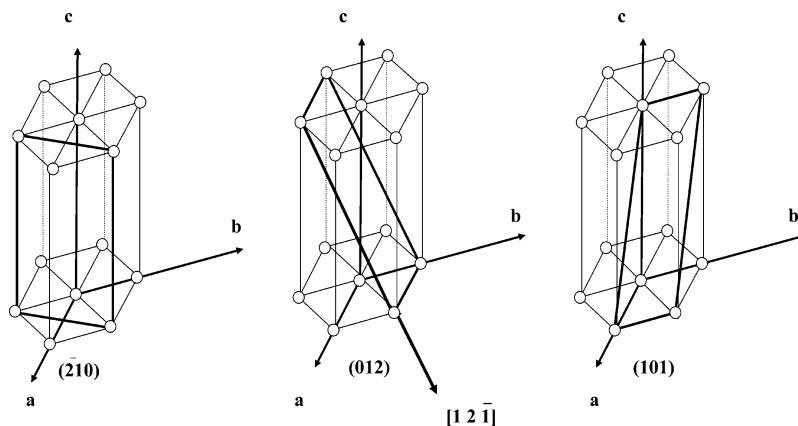


Figure 8. The $(\bar{2}10)$, (012) , and (101) planes of the hexagonal cell. These planes all lie in the $[12\bar{1}]$ zone.

either the 113 (and equivalents) or 300 (and equivalents). The calculated angle between 012 and 113 is 16.8° (on the basis of cell parameters found earlier by X-ray diffraction), which is equal to the measured value on Figure 7, therefore positively identifying this reflection as 113.

Of course, an orthogonal pattern can only be produced by a hexagonal lattice if the crystal lies in other than simple c axis projection. The zone axis $[uvw]$ of the pattern in Figure 7 can be found by the simple relationships

$$u = k_1 l_2 - l_1 k_2$$

$$v = l_1 h_2 - h_1 l_2$$

$$w = h_1 k_2 - k_1 h_2$$

where $(h_1 k_1 l_1)$ and $(h_2 k_2 l_2)$ are two planes lying in this zone. This zone can therefore be identified as $[1\ 2\ \bar{1}]$.

Reflections only occur in electron diffraction if planes are aligned approximately parallel to the incident beam. In the pattern the main planes of interest are $(\bar{2}10)$, (012) , and (101) . These are shown in Figure 8, in the unit cell in real space with the $[12\bar{1}]$ direction also indicated. The parallelism of this direction with the indicated planes is clear. The $(\bar{2}10)$, (012) , and (101) planes therefore must all lie perpendicular to the flat plane of the crystal in Figure 6.

Correlation of the spatial orientation of a crystal with its diffraction pattern (for example, by de-focusing the central electron beam) allows further correlation of the internal crystal structure with the external crystal morphology. This shows that the $(101)/(\bar{1}11)$ equivalent plane lies parallel to the bisector of the apex angle of each arm of the star (Figures 6 and 9). The angle measured between facets at the tips of the arms is $\sim 70^\circ$, which is consistent with the facets being $(\bar{2}10)$ and (123) . These planes are therefore identified as major growth planes in the crystal.

The star morphology has already been recognized as indicative of twinning. It remains to identify the likely twin plane, designated by $(h_t k_t l_t)$. Clearly, the twin plane lies parallel to the crystallographic direction normal to the crystal surface, $[uvw]$. This must therefore satisfy the criterion $h_t u + k_t v + l_t w = 0$. In this case $[uvw]$ is $[12\bar{1}]$. Also, the proposed plane of twinning must lead

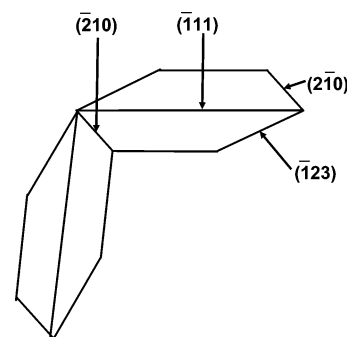


Figure 9. Suggested twinning on the $(\bar{2}10)$ plane. The facets at the tip of the crystal make an interfacial angle of $\sim 70^\circ$ and the angle between the growth direction of the twins is $\sim 95^\circ$.

twins growing at approximately right angles. Twinning on (210) as shown in Figure 9 would satisfy these criteria.

Conclusions

POSS-based materials form a new family of organic–inorganic hybrid, nano-structured materials. In practical applications, the introduction of the inorganic POSS promises to improve fire resistance and to act as mechanical reinforcements. One of the first steps in structure–property studies is the identification and characterization of pertinent structural features. This has been the objective of the present work, using the observation that the crystalline structure of POSS in nano-structured composites is based on the crystal structure of the POSS monomer.

We have shown that POSS monomers decorated with alkyl corner units form a family of materials with structural similarities. POSS units decorated with one norbornyl group in place of an alkyl clearly fit into the same pattern. POSS cages can be treated as spheres which pack hexagonally in ABCA sequence in which spheres in one layer lie above the interstitial spaces in adjacent layers. Corner units occupy space in the structure and prevent “close-packing” of the spheres. When corner units are other than simply hydrogen atoms, the crystal structures have self-similar geometries which are characterized by the same ratio of lattice parameters. In the case where the corner units are hydrogen atoms, spheres pack more closely and stacking of adjacent layers is modified (indicated by a different ratio of lattice parameters).

TEM allows correlation of the crystal structure with external crystal habit. This shows the monomer to crystallize as well-defined, platelike, faceted crystals, showing a high degree of crystallographic regularity.

Acknowledgment. The authors gratefully acknowledge support from the NSF Materials Research Science

and Engineering Center on Polymers at UMass, Amherst (DMR-9809365). E.B.C. also gratefully acknowledges support from the NSF (CAREER Award DMR-0239475). We also acknowledge the assistance of L. Zheng in sample preparation.

CM034308B